Isoscalar giant dipole resonance and nuclear matter incompressibility coefficient

S. Shlomo[1,2] and A. I. Sanzhur[1,3]
[1]*Cyclotron Institute, Texas A&M University, College Station, Texas 77843-3366*
[2]*RIBF Project, Institute of Physical and Chemical Research (RIKEN), 2-1 Hirosawa, Wako, Saitama 351-0198, Japan*
[3]*Institute for Nuclear Research, Kiev 03028, Ukraine*
(Received 11 September 2000; published 18 March 2002)

We present results of microscopic calculations of the strength function $S(E)$ and α-particle excitation cross sections $\sigma(E)$ for the isoscalar giant dipole resonance (ISGDR). An accurate and general method to eliminate the contributions of spurious state mixing is presented and used in the calculations. Our results provide a resolution to the long standing problem that the nuclear matter incompressibility coefficient K deduced from $\sigma(E)$ data for the ISGDR is significantly smaller than that deduced from data for the isoscalar giant monopole resonance.

DOI: 10.1103/PhysRevC.65.044310 PACS number(s): 24.30.Cz, 21.60.Jz, 21.65.+f, 25.55.Ci

I. INTRODUCTION

Studies of compression modes of nuclei are of particular interest since their strength distributions $S(E)$ are sensitive to the value of the nuclear matter incompressibility coefficient K [1,2]. Over the last two decades, a significant amount of experimental work was carried out to identify strength distributions of the isoscalar giant monopole resonance (ISGMR) in nuclei [3]. At present, Hartree-Fock (HF) based random-phase approximation (RPA) calculations for the ISGMR reproduce the experimental data for effective interactions associated with incompressibility $K=210 \pm 20$ MeV [4].

The study of the isoscalar giant dipole resonance (ISGDR) is very important since this compression mode provides an independent source of information on K. Early experimental attempts to identify the ISGDR in ^{208}Pb resulted in a value of $E_1 \sim 21$ MeV for the centroid energy [5,6]. A similar result for E_1 in ^{208}Pb was obtained in recent experiments [7]. Very recent and more accurate data on the ISGDR obtained for a wide range of nuclei [8] seems to indicate that the experimental values for E_1 are smaller than the corresponding HF-RPA results by 3–5 MeV.

It was first pointed out in Ref. [9] that corresponding HF-RPA results for E_1, obtained with interactions adjusted to reproduce the ISGMR data, are higher than the experimental value by more than 3 MeV and thus this discrepancy between theory and experiment raises doubts concerning the unambiguous extraction of K from energies of compression modes.

In this work, we address this discrepancy between theory and experiment by examining the relation between $S(E)$ and the excitation cross section $\sigma(E)$ of the ISGDR obtained by α-scattering. We emphasize that it is quite common in theoretical work on giant resonances to calculate $S(E)$ for a certain scattering operator F, whereas in the analysis of experimental data of $\sigma(E)$ one carries out distorted-wave Born approximation (DWBA) calculations with a certain transition potential. Here we present results of accurate microscopic calculations for $S(E)$ and for $\sigma(E)$ with the folding model (FM) DWBA with transition densities $\rho_t(\boldsymbol{r})$ obtained from HF-RPA calculations and corrected for the spurious state mixing (SSM), using the method first employed by Shlomo and co-workers in Refs. [10,11]. We provide a simple explanation for the long standing discrepancy between theory and experiment concerning the ISGDR.

In Sec. II we present a Green's function based derivation of the projection operator method, used in Refs. [10,11], to eliminate the contributions of the SSM to $S(E)$ and $\rho_t(\boldsymbol{r})$ of the ISGDR obtained in HF-RPA calculations for any operator F. We note that a similar method was first used by Shlomo and co-workers in Ref. [12] in the continuum RPA calculations of $S(E)$ for the overtone of the ISGMR, where the projection scattering operator $(r/R)^2[1-(r/R)^2]$ was employed to eliminate (reduce) the contribution of the ISGMR to $S(E)$. More recently, the method used in our work was employed in the calculation of $S(E)$ of the ISGDR in Refs. [13,14]. This projection method, which is based on the replacement of the scattering operator F with a properly modified operator F_η in the calculation of $S(E)$ and $\rho_t(\boldsymbol{r})$, is quite general and applicable for any value of F and for any numerical method used in carrying out the RPA calculation, such as configuration space RPA, coordinate space (continuum and discretized) RPA, and with and without the addition of smearing. The derivation of the projection scattering operator is given here for the purpose of (i) describing how the method should be implemented correctly and demonstrating its accuracy, (ii) understanding when the method based on subtracting the component of the spurious transition density from that obtained in the HF-RPA calculation is equivalent to the method based on using the projection operator, and (iii) why the first serious attempt of Ref. [15] to correct for the effect of the SSM on $S(E)$ was not successful. In Sec. III we present results and discussion of our accurate microscopic calculations for $S(E)$ and for $\sigma(E)$.

II. FORMALISM

In self-consistent HF-RPA calculation, one starts by adopting specific effective nucleon-nucleon interaction V_{12}, carries out the HF calculation for the ground state of the nucleus, and then solves the RPA equation using the particle-hole (p-h) interaction $V_{p\text{-}h}$ that corresponds to V_{12}. The RPA Green's function G [16,17] is obtained from

$$G = G_0(1 + V_{p\text{-}h}G_0)^{-1}, \tag{1}$$

where G_0 is the free p-h Green's function. For

$$F = \sum_{i=1}^{A} f(\boldsymbol{r}_i), \tag{2}$$

the strength function and transition density are given by

$$S(E) = \sum_n |\langle 0|F|n\rangle|^2 \delta(E - E_n) = \frac{1}{\pi}\mathrm{Im}[\mathrm{Tr}(fGf)], \tag{3}$$

$$\rho_t(\boldsymbol{r},E) = \frac{\Delta E}{\sqrt{S(E)\Delta E}} \int f(\boldsymbol{r}') \left[\frac{1}{\pi}\mathrm{Im}G(\boldsymbol{r}',\boldsymbol{r},E)\right] d\boldsymbol{r}'. \tag{4}$$

Note that $\rho_t(\boldsymbol{r},E)$, as defined in Eq. (4), is associated with the strength in the region of $E \pm \Delta E/2$ and is consistent with

$$S(E) = \left| \int \rho_t(\boldsymbol{r},E) f(\boldsymbol{r}) d\boldsymbol{r} \right|^2 \Big/ \Delta E. \tag{5}$$

In fully self-consistent HF-RPA calculations, the spurious isoscalar dipole ($T=0, L=1$) state (associated with the center-of-mass motion) appears at $E=0$ and no SSM in the ISGDR occurs. However, although not always stated in the literature, actual implementations of HF-RPA (and relativistic RPA) are not fully self-consistent. One usually makes the following approximations: (i) neglecting the two-body Coulomb interactions and spin-orbit interactions in $V_{p\text{-}h}$, (ii) approximating the momentum parts in $V_{p\text{-}h}$, (iii) limiting the p-h space in a discretized calculation by a cutoff energy $E_{p\text{-}h}^{max}$, and (iv) introducing a smearing parameter (i.e., a Lorentzian with $\Gamma/2$). Although the effect of these approximations on the centroid energies of giant resonances is small (less than 1 MeV), the effect on the strength function and the transition density of the ISGDR is quite serious since each of these approximations introduces a SSM in the ISGDR. In the work of Refs. [18,9], the effect of the SSM on $S(E)$ was ignored and was only considered with regard to the energy-weighted sum rule (EWSR) and the derivation of the collective transition density. Similarly, contrary to the statement made in Ref. [13], the effect of the SSM on $S(E)$ was also ignored in Ref. [19].

Let us consider scattering operators [Eq. (2)] with

$$f(\boldsymbol{r}) = f(r)Y_{1M}(\Omega), \quad f_1(\boldsymbol{r}) = rY_{1M}(\Omega), \tag{6}$$

and write $(1/\pi)\mathrm{Im}G$ as the sum of separable terms

$$R(\boldsymbol{r}',\boldsymbol{r},E) = \frac{1}{\pi}\mathrm{Im}G(\boldsymbol{r}',\boldsymbol{r},E) = \sum_a \rho_a(\boldsymbol{r})\rho_a(\boldsymbol{r}'). \tag{7}$$

Note that the energy dependence of $R(\boldsymbol{r}',\boldsymbol{r},E)$ is included in ρ_a. In the case of a well-defined resonance or in a discretized continuum calculation, the sum in Eq. (7) has only one term. In this case ρ_a is proportional to the transition density associated with the resonance and may contain a spurious state contribution. In general, due to the smearing with $\Gamma/2$, the sum in Eq. (7) may contain quite a few terms. We now write ρ_a as

$$\rho_a(\boldsymbol{r}) = \rho_{a3}(\boldsymbol{r}) + \rho_{a1}(\boldsymbol{r}), \tag{8}$$

where $\rho_{a1}(\boldsymbol{r})$ is due to SSM, and ρ_{a3}—associated with the ISGDR—fulfills the center-of-mass condition (for all values of a)

$$\langle f_1\rho_{a3}\rangle = \int f_1(\boldsymbol{r})\rho_{a3}(\boldsymbol{r})d\boldsymbol{r} = 0. \tag{9}$$

From Eqs. (7) and (8) we have in an obvious notation

$$R = R_{33} + R_{31} + R_{13} + R_{11}, \tag{10}$$

where $R_{ij} = \Sigma\rho_{ai}(\boldsymbol{r})\rho_{aj}(\boldsymbol{r}')$, and the required $S(E)$ and ρ_t can be obtained from R_{33} using Eqs. (4) and (5) with f. Since R_{33} is not known, we look for a projection operator that projects out $\rho_{a1}(\boldsymbol{r})$,

$$F_\eta = \sum_{i=1}^{A} f_\eta(\boldsymbol{r}_i) = F - \eta F_1 \ , \tag{11}$$

where $f_\eta = f - \eta f_1$. Using Eqs. (9) and (10) we have

$$S_\eta(E) = \langle f_\eta R f_\eta\rangle = \langle fR_{33}f\rangle + 2\langle fR_{31}f_\eta\rangle + \langle f_\eta R_{11}f_\eta\rangle. \tag{12}$$

Note that $\langle f_\eta R_{11} f_\eta\rangle$ is minimum for

$$\eta = \langle fR_{11}f_1\rangle/\langle f_1R_{11}f_1\rangle = \sum \langle f\rho_{a1}\rangle\langle f_1\rho_{a1}\rangle/\sum \langle f_1\rho_{a1}\rangle^2, \tag{13}$$

and for the last two terms in Eq. (12) to vanish we must have

$$\langle f\rho_{a1}\rangle = \eta\langle f_1\rho_{a1}\rangle \quad \text{for all } a. \tag{14}$$

The condition (14) holds in case Eq. (7) has only one term, occurring in a discretized calculation without smearing or in a configuration space calculation. It also holds in case all $\rho_{a1}(\boldsymbol{r})$ are proportional to the same transition density, i.e., the coherent spurious state transition density [20]

$$\rho_{a1}(\boldsymbol{r}) = \alpha_a\rho_{ss}(\boldsymbol{r}) = \alpha_a \frac{\partial\rho_0}{\partial r} Y_{1M}(\Omega), \tag{15}$$

where ρ_0 is the ground state density of the nucleus. The value of η associated with ρ_{ss} is then given by

$$\eta = \langle f\rho_{ss}\rangle/\langle f_1\rho_{ss}\rangle. \tag{16}$$

To determine ρ_t for the ISGDR we first use Eqs. (4), (7), (8), (9), and (14) with F_η and obtain

$$\rho_\eta(\boldsymbol{r}) = \frac{\Delta E}{\sqrt{S_\eta(E)\Delta E}} \sum c_a[\rho_{a3}(\boldsymbol{r}) + \rho_{a1}(\boldsymbol{r})], \tag{17}$$

with $c_a = \langle f_\eta\rho_{a3}\rangle$. To project out the spurious term from Eq. (17), we make use of Eq. (9) with $\rho_{a1} = \alpha_a\rho_{ss}$ and obtained

$$\rho_t(\boldsymbol{r}) = \rho_\eta(\boldsymbol{r}) - \alpha\rho_{ss}, \quad \alpha = \langle f_1\rho_\eta\rangle / \langle f_1\rho_{ss}\rangle. \tag{18}$$

It is important to emphasize that by using f_η in Eq. (5) with $\rho_t(\boldsymbol{r})$ from Eq. (18), one obtains the required $S_\eta(E)$. This is due to the fact that the averaging process in Eq. (17) was carried out using F_η and not F. Use of F in Eq. (4) may produce erroneous results for $\rho_t(\boldsymbol{r})$ in Eq. (18) in case there are several terms in Eq. (7).

We now limit our discussion to the operator $F_3 = \Sigma_{i=1}^{A} f_3(\boldsymbol{r}_i)$, where $f(\boldsymbol{r}) = f_3(\boldsymbol{r}) = r^3 Y_{1M}(\Omega)$. For this operator, the value of η associated with the spurious transition density (15) is

$$\eta = \frac{5}{3}\langle r^2\rangle. \tag{19}$$

We note that the values of η obtained for ρ_a associated with single p-h transitions in the $1\hbar\omega$ region and the RPA results for the spurious state ρ_t differ from that of Eq. (19) by less than 20% [21].

III. RESULTS AND DISCUSSION

We have carried out numerical calculations for the $S(E)$, $\rho_t(\boldsymbol{r})$, and $\sigma(E)$ within the FM-DWBA-HF-RPA theory. We used the SL1 Skyrme interaction [22], which was associated with $K = 230$ MeV, and carried out HF calculations using a spherical box of $R = 15$ fm. For the RPA calculations we used the Green's function approach with mesh size $\Delta r = 0.3$ fm and p-h maximum energy of $E_{p\text{-}h}^{max} = 150$ MeV (we included particle states with principle quantum number up to 12), since it is well known that in order to extract accurate $\rho_t(\boldsymbol{r})$, $E_{p\text{-}h}^{max}$ should be much larger than the value required ($E_{p\text{-}h}^{max} \sim 50$ MeV) to recover the EWSR. Since in our calculations we also neglected the two-body Coulomb interactions and spin-orbit interactions, the spurious state energies differed from 0 by a few MeV. We, therefore, renormalized the strength of the $V_{p\text{-}h}$ by a factor (0.99 and 0.974 for ^{116}Sn and ^{208}Pb, respectively), to place the spurious state at $E = 0.2$ MeV. We have included a Lorentzian smearing ($\Gamma/2 = 1$ MeV) and corrected for the SSM as described above. We carried out the FM-DWBA calculations for $\sigma(E)$ using a density dependent Gaussian α-nucleon interaction with parameters adjusted to reproduce the elastic cross section, with ρ_0 and ρ_t from HF-RPA (see Ref. [25] for details of the FM-DWBA-HF-RPA calculations of the cross sections).

Using the operator $f = r^2$ for the ISGMR, we calculated the corresponding $S(E)$ for E up to 60 MeV. We recovered 100% of the corresponding EWSR and obtained the values of 17.09 and 14.48 MeV for the centroid energy of the ISGMR in ^{116}Sn and ^{208}Pb, respectively. The corresponding recent experimental values are 16.07 ± 0.12 and 14.17 ± 0.28 MeV, respectively [23].

The first serious attempt to correct for the effect of the SSM on $S(E)$ and ρ_t, associated with $f_3(\boldsymbol{r})$, was presented in Ref. [15]. However, the method adopted in this work is not accurate and leads to a strong reduction in the ISGDR strength at low energies. This is due to the fact that the transition densities associated with the operators f_1 (spurious state) and f_3, obtained by using the method adopted in Ref. [15], coincide in the case of a well-defined resonance, which results in the vanishing of the strength function. To understand how the method should be implemented correctly and to demonstrate its accuracy, we present results of strength functions associated with the scattering operators f_1, f_3, and f_η in Figs. 1 and 2. In Fig. 1, we show the results of the $ES_3(E)$ and $ES_1(E)$ for ^{116}Sn, obtained directly from the RPA Green's function by using Eq. (3) with f_3 and f_1, respectively. Note that from Eqs. (9) and (10), we get $S_1(E)$

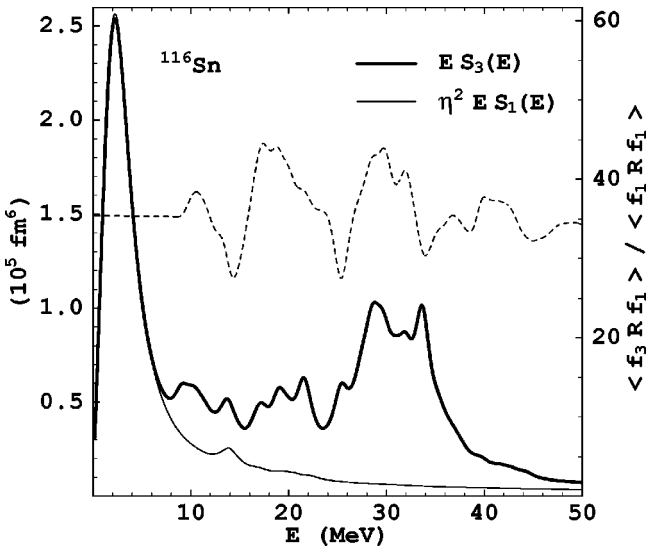

FIG. 1. Energy-weighted strength functions for ISGDR in ^{116}Sn, obtained from Eq. (3) for the scattering operators f_3 (thick line) and f_1 (thin line) with $\eta = \frac{5}{3}\langle r^2\rangle = 35.6$ fm^2. Also shown is the ratio $\langle f_3 R f_1\rangle / \langle f_1 R f_1\rangle$ (dashed line).

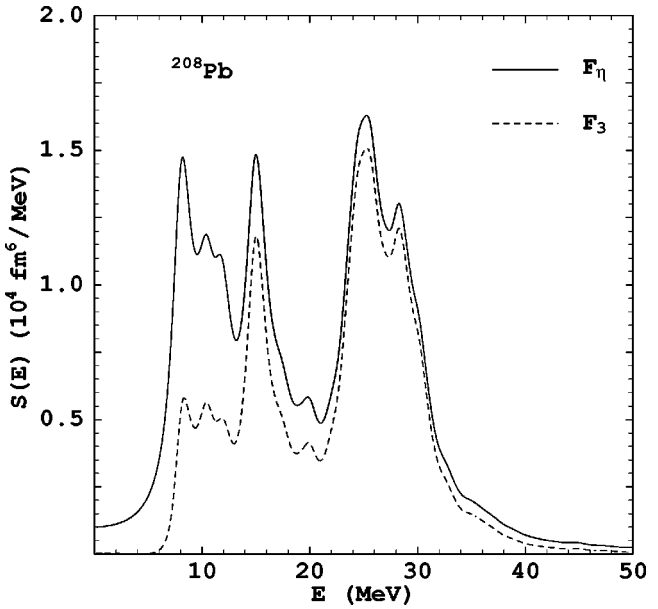

FIG. 2. Strength functions for the ISGDR in ^{208}Pb obtained from Eqs. (4), (18), and (5), using f_3 (dashed line) and $f_\eta = f_3 - \eta f_1$ (solid line), with $\eta = 52.1$ fm^2.

$=\langle f_1 R_{11} f_1\rangle = \Sigma \langle f_1 \rho_{a1}\rangle^2$, which provides a measure of the contribution of the SSM to $S_3(E)$. The large contribution from the Lorentzian tail of the spurious state is clearly seen in the figure. Also shown in Fig. 1 is the ratio $\langle f_3 R f_1\rangle / \langle f_1 R f_1\rangle$. At low energy this ratio is very close to η, reflecting the fact that the transition density at the spurious state energy is close to that of Eq. (15) [21]. At higher energies, this ratio exhibits fluctuations due to the non-negligible terms R_{31} [Eq. (10)].

Figure 2 shows the results of strength functions for the ISGDR in ^{208}Pb obtained by first calculating the ''corrected'' transition density and then using Eq. (5). The solid line describes the result obtained using the scattering operator f_η in Eq. (4) and then employing Eq. (18) to determine the corrected transition density used in Eq. (5). As pointed out after Eq. (18), this result (solid line) coincides with the correct strength function $S_\eta(E)$, obtained directly from Eq. (3) using the projection operator f_η, which is free of the SSM contribution. The dashed line describes an erroneous result obtained using the scattering operator f_3 in Eq. (4) and then using Eqs. (18) and (5). This erroneous result (dashed line) clearly demonstrates that although Eq. (18) was employed to ''correct'' for the SSM, we obtained erroneous transition densities (and the strength function) by using f_3 in Eq. (4) (instead of f_η) in determining the ''corrected'' transition densities. To avoid confusion, we emphasize here that this result (dashed line) is also different from the incorrect strength function $S_3(E)$ (see the thick line of Fig. 1), deduced directly from Eq. (3) using f_3. We also find that while using f_3, the excitation strengths obtained for certain states (dashed line) are sensitive to the value of Γ. The result obtained with f_3 coincides with that obtained with f_η for $\Gamma \to 0$, as expected, since in this case Eq. (7) has only one term. Thus the results in Figs. 1 and 2 show that it is important to use the projection operator f_η in the calculation of both the strength function and the transition density of the ISGDR. It is also clear from Figs. 1 and 2 that even in fully self-consistent HF-RPA calculations, one should adopt the projection operator f_η in determining the ISGDR strength function and transition density if a nonzero value of Γ is used. Only in discretized RPA calculation of $S(E)$ and ρ_t of the ISGDR, one may also use f_3 in Eqs. (4) and (18) and correct for the SSM contribution before the smearing process.

As seen from the solid line of Fig. 2, our results for the ISGDR, $S_\eta(E)$, indicate two main components in agreement with the experimental observation [24]. Similar results were obtained for other nuclei and in other calculations [10,13,14,21,26]. In Fig. 3 we present results of microscopic calculations of the excitation cross section of the ISGDR, E1T0, in ^{116}Sn by 240 MeV α-particle scattering, carried out within the FM-DWBA. For details of the FM-DWBA-HF-RPA calculations and the procedure for extracting the strength distribution from the cross section, see Ref. [25]. The middle panel of the figure shows the double differential E1T0 cross sections obtained with RPA transition density (i.e., our ''experimental'' data), calculated at the first maxima of the E1T0 angular distributions. In the lower panel, we show the E1T0 cross sections found using the RPA transition density (solid line) and with the collective model

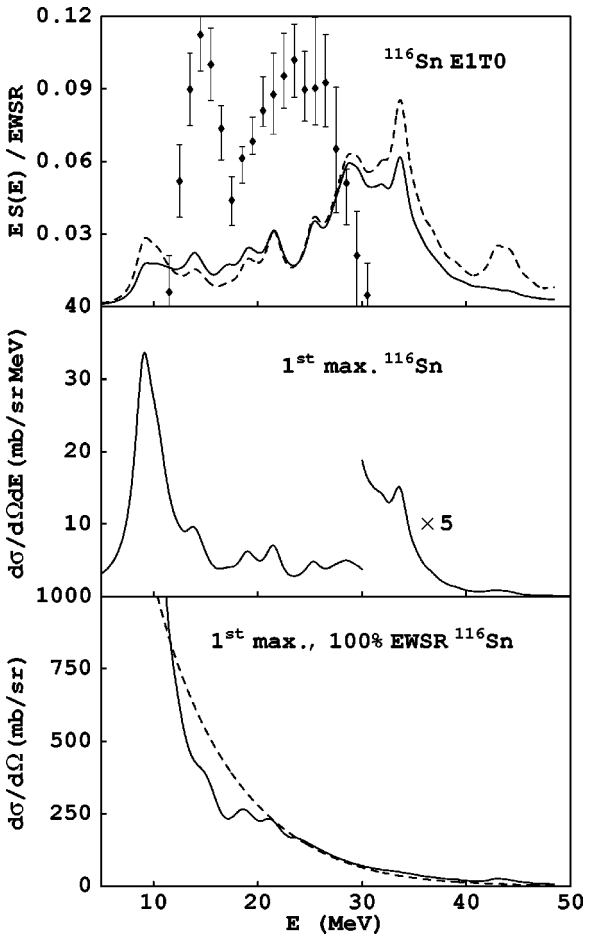

FIG. 3. The ISGDR in ^{116}Sn. The middle panel: maximum double differential cross section obtained from ρ_t (RPA). The lower panel: maximum cross section obtained with ρ_{coll} (dashed line) and ρ_t (solid line) normalized to 100% of the EWSR. Upper panel: the solid and dashed lines represent the ratios of the middle panel curve with the solid and dashed lines of the lower panel, respectively. The experimental data points shown in the upper panel are taken from Ref. [24].

E1T0 transition density $\rho_{coll}(r)$ [2,19] (dashed line), normalized to 100% of the E1T0 EWSR. The dashed line in the upper panel of the figure is the ratio of the curve in the middle panel and the one in the lower panel. It represents the fraction of the E1T0 EWSR per unit energy reconstructed from our ''experimental'' cross sections. The solid line in the upper panel shows the actual fraction of the E1T0 EWSR per unit energy as obtained from the HF-RPA calculations. The experimental data points shown in the upper panel are taken from Ref. [24].

It can be seen from Fig. 3 (top panel) that the cross section analysis based on using $\rho_{coll}(r)$ tends to overestimate the E1T0 EWSR by at least 10%. Difference in shape between the collective model and the microscopic transition densities can also lead to deviation of the ISGDR centroid energy deduced from the reconstructed strength distribution from the actual centroid energy obtained from microscopic calculations. This shift, however, is of the order of a few percent and thus not very significant. Similar results were

obtained for other nuclei [21].

It is seen from the upper panel of Fig. 3 that our HF-RPA calculations show significant strength distribution in the region of 5–50 MeV excitation energy as compared to the smaller experimental data region of 12–32 MeV [24]. The experimental value for the centroid energy of the upper component is 23 MeV, which is smaller than the HF-RPA value of 28 MeV (for the region above 16 MeV) by 5 MeV. However, it is clearly seen from the upper panel of Fig. 3 that the experimental values of the fraction of the EWSR are significantly larger than the HF-RPA results by about a factor of 3. The experimental data overestimate the EWSR by about 40%, in disagreement with our calculations that predict less than half of the EWSR in the experimental region of 12–32 MeV. A very important result of our calculation which can be seen from the middle panel of Fig. 3 is the following. The maximum cross section for the ISGDR compression mode (the region of excitation energy $E=20-40$ MeV) is flat (as a function of E), small, and decreases at high E to below the experimental sensitivity of about 2 mb/sr/MeV for E larger than 34 MeV (29 MeV for ^{208}Pb). The region of E above 34 MeV and the region of E above 30 MeV (the maximum experimental excitation energy) contain more than 20% and 40% of the EWSR, respectively. We note that 20% of the EWSR in the region of E above 34 MeV increases the centroid energy of the ISGDR by about 2.5 MeV (see also Ref. [21]). Thus, the results shown in the middle panel of Fig. 3 point out to the existence of a missing strength in the experimental data and the results shown in the upper panel indicate that less than half of the EWSR was seen experimentally. This missing strength at high excitation energy provides a resolution of the discrepancy between theory and experiment concerning the centroid of the ISGDR. More sensitive experiments and/or with higher α-particle energy are thus needed.

In summary, we described and applied an accurate and general method to eliminate the SSM contributions from $S(E)$ and ρ_t. Our results indicate: (i) existence of non-negligible ISGDR strength at low energy and (ii) accurate determination of the relation between $S(E)$ and $\sigma(E)$ resolves the long standing problem of the conflicting results obtained for K, deduced from published experimental data $\sigma(E)$ for the ISGDR and data for the ISGMR.

ACKNOWLEDGMENTS

We thank Professor A. Arima and Professor I. Hamamoto for interesting discussions. This work was supported in part by the U.S. Department of Energy under Grant No. DOE-FG03-93ER40773.

[1] A. Bohr and B. Mottelson, *Nuclear Structure* (Benjamin, London, 1975), Vol. II, Chap. 6.
[2] S. Stringari, Phys. Lett. **108B**, 232 (1982).
[3] S. Shlomo and D.H. Youngblood, Phys. Rev. C **47**, 529 (1993).
[4] J.P. Blaizot, Phys. Rep. **64**, 171 (1980).
[5] H.P. Morsch, M. Rogge, P. Turek, and C. Mayer-Boricke, Phys. Rev. Lett. **45**, 337 (1980).
[6] C. Djalali, N. Marty, M. Morlet, and A. Willis, Nucl. Phys. **A380**, 42 (1982).
[7] B. Davis, *et al.*, Phys. Rev. Lett. **79**, 609 (1997).
[8] H.L. Clark, Y.-W. Lui, D.H. Youngblood, K. Bachtr, U. Garg, M.N. Harakeh, and N. Kalantar-Nayestanski, Nucl. Phys. **A649**, 57c (1999).
[9] T.S. Dumitrescu and F.E. Serr, Phys. Rev. C **27**, 811 (1983).
[10] A. Kolomiets, O. Pochivalov, and S. Shlomo, Cyclotron Institute, Texas A&M University, III-1, 1999 (unpublished).
[11] M.L. Gorelik, S. Shlomo, and M.H. Urin, Phys. Rev. C **62**, 044301 (2000).
[12] S.E. Muraviev, I. Rotter, S. Shlomo, and M.H. Urin, Phys. Rev. C **59**, 2040 (1999).
[13] G. Colo, N. Van Giai, P.F. Bortignon, and M.R. Quaglia, Phys. Lett. B **485**, 362 (2000).
[14] D. Vretenar, A. Wandelt, and P. Ring, Phys. Lett. B **487**, 334 (2000).
[15] I. Hamamoto, H. Sagawa, and X.Z. Zhang, Phys. Rev. C **57**, R1064 (1998).
[16] G.F. Bertsch and S.F. Tsai, Phys. Rep., Phys. Lett. **18**, 125 (1975).
[17] S. Shlomo and G.F. Bertsch, Nucl. Phys. **A243**, 507 (1975).
[18] T.J. Deal, Nucl. Phys. **A217**, 210 (1973).
[19] N. Van Giai and H. Sagawa, Nucl. Phys. **A371**, 1 (1981).
[20] G.F. Bertsch, Suppl. Prog. Theor. Phys. **74**, 115 (1983).
[21] S. Shlomo and A.I. Sanzhur, nucl-th/0011098; S. Shlomo, Pramana, J. Phys. **57**, 557 (2001); S. Shlomo *et al.* (to be published).
[22] K.-F. Liu, H.-D. Lou, Z.-Y. Ma, and Q.-B. Shen, Nucl. Phys. **A534**, 1 (1991); **A534**, 25 (1991).
[23] D.H. Youngblood, H.L. Clark, and Y.-W. Lui, Phys. Rev. Lett. **82**, 691 (1999).
[24] H. L. Clark, Y.-W. Lui, and D. H. Youngblood, Cyclotron Institute, Texas A&M University, I-9, 1999; I-17, 2000; Phys. Rev. C **63**, 031301(R) (2001).
[25] A. Kolomiets, O. Pochivalov, and S. Shlomo, Phys. Rev. C **61**, 034312 (2000).
[26] J. Piekarewicz, Phys. Rev. C **62**, 051304(R) (2000).